JIDC | THE JOURNAL OF INFECTION IN DEVELOPING COUNTRIES

Original Article

E. coli-synthesized selenium nanoparticles suppress *phoP* and *bapA* gene expression in *S. enterica* isolated from human blood

Sarab M Kadhem[1], Nawal J Shanyoor[2], Zainab F Shubrem[3,4], Huda A Abd[5]

[1] *College of Dentistry, Aliraqia University, Baghdad, Iraq*
[2] *Department of Biology, College of Science, Mustansiriyah University, Baghdad, Iraq*
[3] *National Center for Educational Laboratories, Medical City, Ministry of Health, Baghdad, Iraq*
[4] *Al-Wastiy Teaching Hospital, Baghdad, Iraq*
[5] *University of Information Technology and Communications (UOITC), Baghdad, Iraq*

Abstract

Introduction: Typhoid fever is caused by *Salmonella enterica*, which is a chronic health problem in endemic areas due to multidrug resistance and biofilm development. The stress adaptation and virulence regulatory gene *phoP* and the biofilm-associated gene *bapA* may represent molecular targets for anti-virulence interventions. In this study, *S. Typhi* isolates from blood samples were characterized for their antimicrobial sensitivity and biofilm formation, and the molecular impact of biosynthesized selenium nanoparticles (SeNPs) on *phoP* and *bapA* expression was assessed.

Methodology: Biochemical analyses and 16S rRNA polymerase chain reaction (PCR) were performed on 92 blood samples identified 35 *S. Typhi* isolates. Antimicrobial susceptibility was evaluated by standard protocols. Biofilm-formation capacity was determined. SeNPs were obtained from *E. coli* by biological synthesis according to ultraviolet–visible (UV-vis) spectroscopy, Fourier-transform infrared (FTIR) spectroscopy, and X-ray diffraction (XRD) analyses; at concentrations of 12.5–100 µg/mL. Differences in gene expression were quantified by quantitative reverse transcription real-time PCR.

Results: All the isolates were resistant to ampicillin and ceftriaxone; susceptible to meropenem, ertapenem, trimethoprim–sulfamethoxazole, chloramphenicol, and tetracycline; and had variable sensitivity to ciprofloxacin. The isolates induced strong (57.1%) and moderate (40%) biofilm formation. The production of *phoP* and *bapA* were significantly inhibited by SeNPs treatment in a concentration-dependent manner, with maximal inhibition at 100 µg/mL ($p = 0.0001$); and exhibited a significant positive correlation for both genes (R = 0.899).

Conclusions: Biosynthesized SeNPs effectively downregulate key virulence determinants in antibiotic-resistant *S. Typhi*, supporting their potential as adjunctive or alternative therapies capable of decelerating pathogenicity and biofilm-associated persistence.

Key words: selenium; nanoparticles; *E. coli*; *Salmonella*; *phoP* gene; *bapA* gene.

J Infect Dev Ctries 2026; 20(8):1133-1144. doi:10.3855/jidc.22789

(Received 19 December 2025 – Accepted 09 April 2026)

Introduction

Nanoscience and nanotechnology are fast-evolving interdisciplinary fields that concern themselves with the study of structures, devices, and systems at a nanometer scale (1–100 nm) and extending their scope of activity. All new properties and functions for such materials are demonstrated because the structure of atoms is perfectly laid out [1]. The trace element selenium (Se) is of high biomedical interest in biological system chemistry as it has profound and crucial antioxidant, immune, and enzymatic action. One notable achievement exploiting these roles is the production of selenium nanoparticles (SeNPs). Specifically, SeNPs, due to their special nanoscale properties, provide enhanced biological activity with less toxicity in comparison to inorganic and organic selenium compounds; and this makes them very attractive for new therapeutic and biomedical applications [2,3]. Classical chemical and physical methods for the synthesis of nanoparticles (NPs) are frequently limited in application towards biomedical-based applications due to their high cost and use of toxic reagents. In contrast, biological synthesis or "green synthesis" has arisen as a promising, sustainable and efficient alternative using biological agents, such as microorganisms, for the synthesis of stable NPs [4]. *Escherichia coli* is well-known for its remarkable capability of reducing selenite ions (Na_2SeO_3) to stable SeNPs [5].

Salmonella enterica is well documented as one of the most significant foodborne pathogens affecting global public health. Its pathogenicity is essentially driven by the activity of virulent factors for survival within the host and the consequent disease promotion [6]. The *S. enterica bapA* gene encodes a large secreted surface-associated protein, bapA. Biofilm formation, adhesion, and host colonization are all significantly dependent on this protein. Earlier studies have demonstrated the destruction of biofilm formation as a

result of deletion of *bapA*, and this strongly reduced bacterial colonization and invasion in animal models of infection; conversely, overexpression of *bapA* enhanced biofilm biomass [7]. A further indication of the broader biofilm-regulatory network of bapA is that, bapA is located on the surface of a cell and is lightly associated with it. Additionally, the transcriptional regulator CsgD can regulate its expression along the lines of curli fimbriae and cellulose biosynthesis. Recent advances have revealed the structural features of *bapA*. bapA consists of tandem BIg (Ig-like) domains, whose folding and stability depend on calcium binding [8]. Such structural reinforcements not only preserve the stability of the biofilm matrix of the genome, but also enhance bacterial persistence for longer under environmental and host-associated stresses. Together, these findings suggest that bapA plays a central role in biofilm formation and virulence outcomes following infection with *S. enterica*, and environmental persistence influences the potential for bacterial pathogenesis.

The two-component system of PhoP/PhoQ in *S. enterica* consists of the sensor kinase PhoQ, which responds to environmental signals such as low magnesium, acidic pH, osmotic stress, or antimicrobial peptides; and activates the response regulator PhoP. PhoP can switch on when it is phosphorylated [9]. After PhoP achieves phosphorylation, a broad-range gene expression system is established by which environmental adaptation, and resistance to stress and virulence can be advanced [10]. Thus, genes located in the *Salmonella* pathogenicity islands (SPI-1 or SPI-2) are regulated. In addition to its classical function in stress adjustment, phoP has also been demonstrated to exert a direct modulatory effect on virulence determinants. It also induces expression of an operon of *orgB* and *orgC*, expressed in SPI-1, indicating the connection of environmental self-sustaining pathways and invasion-associated networks. Furthermore, the PhoP/PhoQ system is regulated by RstA/RstB and SsrB/SsrA, two other proteins that alter bacterial response against an ever-evolving host environment [11]. In total, these properties characterize phoP as a key regulator integrating stress response and virulence, allowing for a boost in *Salmonella* colonization and infection capability. However, despite extensive characterization of SeNPs in terms of their physicochemical properties, their mechanism of modulating the genetic regulation of the virulence determinants in *S. enterica* is yet to be defined.

The aim of this study was to biosynthesize SeNPs in *E. coli*, characterize these particles using high-fidelity laboratory methods, and evaluate how varying concentrations of SeNPs influence the expression levels of the *phoP* and *bapA* genes in *S. enterica.*

Methodology

Characteristics of bacterial isolates

A total of 92 clinical peripheral blood samples were harvested aseptically and analyzed by microbiological methods. The patients were prospectively recruited based on clinical suspicion of typhoid fever with persistent fever and associated gastrointestinal symptoms. Only patients in the acute symptomatic phase were included, while anyone previously diagnosed with chronic or recurrent infections was excluded. The samples were initially inoculated into an enrichment and selective culture media (xylose lysine deoxycholate, (XLD) agar and *Salmonella–Shigella* (SS) agar) and incubated at 37 °C to allow for bacterial growth. Colony morphological data suggestive of *Salmonella* (non-lactose fermenting, hydrogen sulfide–producing colonies) were stained with Gram stain and a panel of biochemical tests including triple sugar iron (TSI) agar, urease, citrate utilization, and motility assays to substantiate the phenotypic identity. Molecular confirmation was performed by polymerase chain reaction (PCR) amplification of the 16S rRNA gene using standard universal primers (F: AGAGTTTGATCMTGGCTCAG, R: GGTTACCTTGTTACGACTTACTT). A total of 35 isolates were identified and determined to be *S. enterica* subsp. *Typhi* based on the combined culture, biochemical, and molecular results of the 92 blood samples tested.

Ethical approval

The study, including both the descriptors and the consent form, was reviewed and approved by the College of Science Research Ethics Committee (College of Science, Mustansiriyah University) and approved (approval ID BCSMU/1724/00073M) in June 2024. Written informed consent was obtained from all subjects.

Antimicrobial susceptibility testing

Antimicrobial sensitivity testing of the *Salmonella* isolates was carried out according to the Clinical and Laboratory Standards Institute (CLSI) standards, and the isolates were categorized into three classes: sensitive (S), intermediate (I), or resistant (R) [12]. The antimicrobial titer plate method was used following the protocol described by Agarwal *et al.* [13]. The antibiotic disks were imported from Liofilchem (Roseto

degli Abruzzi, Italy) and used at concentrations of meropenem (MEM) 10 µg, ciprofloxacin (CIP) 5 µg, ertapenem (ERT) 10 µg, trimethoprim-sulfamethoxazole (STX) 25 µg, ampicillin (AM) 10 µg, ceftriaxone (CRO) 30 µg, chloramphenicol (C) 30 µg, and tetracycline (TE) 25 µg. Thus, a wide range of drug classes and mechanisms of action were used in bacterial susceptibility assessment. Isolates resistant to more than 3 antibiotics were described as multidrug resistant (MDR).

Biofilm formation

Biofilm generation by *Salmonella* isolates was tested by both qualitative and quantitative methods. Colonies showing black, dry, and coarse appearance were classified as slime or biofilm positive; red or smooth colonies were interpreted as weak (non-substrate) or non-biofilm producing colonies. The biofilm was classified on Congo red agar (CRA) [14]. Quantitative evaluation was conducted with a microtiter plate assay in which all the wells were inoculated with 100 µL of bacteria suspension in nutrient broth and incubated at 37 °C for 24–48 hours. Non-adherent cells were removed from the plate following incubation, and the remaining biofilm was stained with 1% crystal violet. The remaining dye was quantified by microplate reader measurement of absorbance at 570 nm.

The biofilm-forming capacity was classified according to the optical density cutoff (ODc) which was 3 standard deviations above the negative control mean optical density [15]. Consequently, the isolates were identified as non-producers ($OD \leq ODc$), weak producers ($ODc < OD \leq 2 \times ODc$), moderate producers ($2 \times ODc < OD \leq 4 \times ODc$), or strong producers ($OD > 4 \times ODc$). All the experiments were conducted in triplicate with biological replicates for reproducibility and methodological consistency, so that there was a standardized basis to analyze biofilm formation among the isolates.

Preparation of SeNPs using E. coli

SeNPs were biosynthesized using *E. coli* isolates. The stock Na_2SeO_3 solution consisted of 0.425 g Na_2SeO_3 + 25 mL sterile distilled water. This stock was filtered through a 0.22 µm syringe filter to obtain different working concentrations of the solution (25, 50, 100 mM). Out of the 50 isolates, 20 *E. coli* strains were chosen based on their high selenium tolerance and biosynthetic efficiency. Selection was based on the color change of the medium from colorless to red and the successful reduction of Na_2SeO_3 to SeNPs. These isolates were optimized for conditions affecting SeNP biosynthesis, including reaction time (24 and 48 hours), Na_2SeO_3 concentration (25, 50, 100 mM), pH (5–9), and shaker speed (130–160 rpm). To prepare SeNPs, a single colony of *E. coli* was inoculated in nutrient broth (5 mL) and incubated for 24 hours at 160 rpm. The culture was further added to 100 mL nutrient broth with 2 mL filter-sterilized Na_2SeO_3 (100 mM). The pH was adjusted to 8, and the cultures were incubated for 48 hours at 37 °C with shaking at 160 rpm. During this time, the solution color gradually changed from yellow to red, and this was indicative of the formation of SeNPs. SeNPs were separated and purified by centrifugation at 10,000 rpm for 10 minutes. The pellets were washed twice with 0.9% NaCl and resuspended in Tris-HCl buffer (pH 8.2). Ultra sonication was performed at 100 W for 10 minutes, and then filtered through 0.22 µm syringe filters. The precipitate of SeNPs was then washed with ethanol and deionized water, and then dried at 45–50 °C in a hot air oven.

Characterization of SeNPs

The synthesized SeNPs were characterized by various analytical methods to assess their structure and functional properties:

UV-visible (UV-vis) spectroscopy

The surface plasmon resonance (SPR) and absorption spectra of biologically synthesized SeNPs were resolved using a UV-vis spectrophotometer in the 200–1000 nm band.

Fourier transform infrared spectroscopy (FTIR)

FTIR analysis was performed to investigate the interaction of the structure of biomolecules (proteins mainly) and SeNPs and to identify the functional groups to be used for the synthesis of the nanoparticles between 4000 and 400 cm^{-1}.

X-ray diffraction (XRD)

The crystalline structure of SeNPs and the crystallite size were assessed by XRD analysis. The average crystallite size (D) was determined using the Debye–Scherrer formula and this provided insight into the scale of the synthesized particles at the nanoscale.

Molecular effect of SeNPs on phoP and bapA genes

Sample preparation

Nanomaterial dilutions for molecular analysis were prepared with a solution of brain heart infusion (BHI) broth with sucrose (2 g/100 mL) as a diluent. Serial 2-fold dilutions were prepared with final concentrations of 100, 50, 25, and 12.5 µg/mL. The treatment mixtures,

Table 1. Complementary DNA synthesis reaction components and thermal conditions.

Reaction component				Thermal profile	
Component	**Volume (µL)**	**Component**	**Volume (µL)**	**Temperature (°C)**	**Duration**
2× ES Reaction Mix	10	Random primer (N9)	1	25	10 min
gDNA Remover	1	RNase-free water	3	42	15 min
Anchored oligo(dT)	1	EasyScript RT/RI enzyme mix	1	85	5 sec
Total RNA		**5 µL**			

*ES: EasyScript ®

totaling 5 mL each, included 2 mL sucrose-enriched BHI medium, 0.5 mL bacterial suspension, and 2.5 mL of the same nanomaterial dilution using overnight bacterial cultures grown in BHI broth. The mixtures were incubated overnight under standard conditions, and then the bacterial cells were harvested by centrifugation. The pellets were placed in sterile Eppendorf tubes; resuspended in 1 mL of TRIzol reagent, and stored at − 20 °C until RNA extraction.

RNA extraction

Total RNA was generated and extracted with the TransZol Up Plus RNA Kit (ER501-01, TransGen Biotech, Beijing, China) as per the protocol and procedures described previously provided by the manufacturer [16]. In short, bacterial pellets were lysed with TransZol reagent, together with phase separation with chloroform and precipitation with ethanol. The RNA-rich phase was purified by washing in spin columns, eluted in RNase-free water, and determined using a Nanodrop spectrophotometer One C (Thermo Fisher Scientific, Waltham, MA, USA) [17]. The purified RNA samples were stored at − 80 °C until use. [Grab your reader's attention with a great quote from the document or use this space to emphasize a key point. To place this text box anywhere on the page, just drag it.]

Complementary DNA synthesis

The EasyScript® One-Step gDNA Removal and cDNA Synthesis SuperMix (Cat. No AE311-02, TransGen Biotech, Beijing, China), which is engineered to eliminate genomic DNA and introduce complementary DNA (cDNA) simultaneously [18], effectively reducing RNA contaminants, was used. The reaction components and thermal profile are indicated in Table 1.

Primers

The primers used in this study were obtained from Macrogen Company, Seoul, South Korea (Table 2). The primers were first provided in lyophilized form and were further dissolved in deionized water to obtain a working concentration of 10 pmol/mL [19]. This preparation of primers allowed for future utilization for downstream molecular purposes.

Gene expression

Gene expression analysis was performed with Quantitative Reverse Transcription Real-Time polymerase chain reaction (RT-qPCR) on TransStart® Top Green qPCR SuperMix (AQ131-01, TransGen Biotech, Beijing, China) following the manufacturer's guidelines. All subsequent steps were performed in a final volume of 20 µL, including 2 µL cDNA template, 1 µL of both forward and reverse primers, 6 µL nuclease-free water, and 10 µL reaction mix. The amplification cycle included initial denaturation at 94 °C for 60 s; and 40 cycles of 94 °C for 10 s, annealing at 56 °C for 15 s, and extension at 72 °C for 20 s. Melting curve analysis was performed from 65 °C to 95 °C with 1 °C/second increments for validation of specificity. All reactions were performed in duplicate to guarantee the reproducibility and reliability of the data.

Statistical analysis

Data analysis was conducted with GraphPad Prism (version 8.0; GraphPad Software, San Diego, CA, USA) and SPSS software (version 26.0; IBM Corp, Armonk, NY, USA). Mean ± standard deviation (Mean ± SD) was calculated for numeric variables. Percentages and numbers were calculated for qualitative variables. *PhoP* and *bapA* gene expression were quantified as a dependent variable using the comparative threshold cycle (ΔΔCt), with *gapA* serving as an endogenous reference gene for normality, whereas

Table 2. Details of the primers.

Gene	Direction	Sequence (5' ---- 3')	Product size (bp)	Primer length	GC%	Tm (°C)	Ta (°C)
phoP	F	TACGGTTACTGCCATCACCA	151	20	50.00	59.99	56
	R	ATGTCCGTATCCTGCCGTAG		20	55.00	59.98	
bapA	F	TGCGCGTACTGGTTGTAGAG	169	20	55.00	60.07	56
	R	TCATCCGGCAGACCTAAATC		20	50.00	60.04	
gap A	F	TACTGTTCACGCGACTACCG	173	20	55.00	59.93	56
	R	GGAACGCCATACCAGTCAGT		20	55.00	60.00	

the *gapA* gene became the endogenous reference gene when normalized. Expression of fold mutations in gene expression was estimated as $2^{\wedge-\Delta\Delta Ct}$. One-way analysis of variance (ANOVA) was conducted for group comparisons, with Duncan's multiple range test used to find significant differences between means. A $p < 0.05$ was considered statistically significant.

Results

Demographic characteristics

Patients with bacterial isolates in blood ranged in age from 5 to 59 years, with a mean of 21.4 years and a median of 14 years. The 95% confidence intervals for both mean (15.889 to 26.911) and median (11.242 to 22.000) further reflect the statistical precision of the age distribution, with the majority of patients falling within the 9–29 years range. The male-female ratio was 15 (42.9%) males to 20 (57.1%) females; there was no significant difference between the two groups. Thus, the distribution of males and females was balanced, with no statistically significant predominance of either gender.

Antimicrobial susceptibility tests

Antimicrobial susceptibility of the *Salmonella isolates* tested were analyzed based on the SIR classification system in which an isolate was described as susceptible (S) if it was inhibited by the antimicrobials at standard dose, intermediate (I) if there was risk of low susceptibility to the antimicrobials or treatment was possible only at high dose, and resistant (R) if the isolate was not inhibited and the antibiotic was likely to be ineffective. The results indicated that all isolates (100%) were resistant (R) to ampicillin and ceftriaxone, showing significant β-lactam resistance. Nevertheless, the MDR criteria were satisfied only by the 25.71% of the isolates exhibiting resistance to ciprofloxacin as well. Complete susceptibility (S) to the selected antibiotics (meropenem, ertapenem, trimethoprim–sulfamethoxazole, chloramphenicol, and tetracycline) was detected for all tested strains, indicating that these compounds represented effective therapeutics. Ciprofloxacin was the exception, with 9 isolates (25.71%) being susceptible, 18 isolates (51.43%) with intermediate susceptibility, and 9 isolates (25.71%) with resistance; suggesting that fluoroquinolone sensitivity sharply decreased. This antimicrobial profile emphasizes the existence of MDR, especially against β-lactams, and emphasizes the emergence of diminished ciprofloxacin efficacy in *Salmonella* isolates (Table 3).

Figure 1. UV–vis absorption spectrum of biosynthesized selenium nanoparticles (SeNPs).

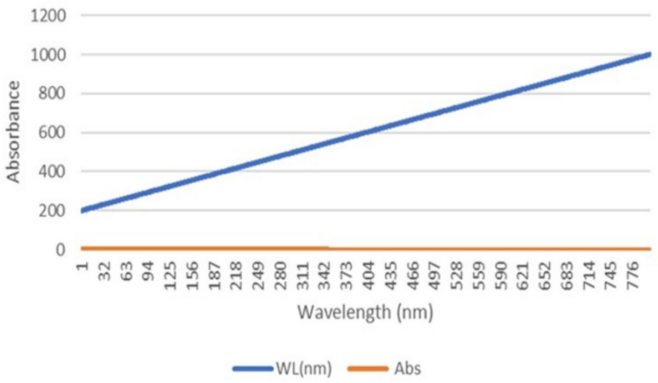

Figure 2. SEM micrograph of amorphous biogenic selenium nanoparticles (SeNPs) synthesized by E. coli.

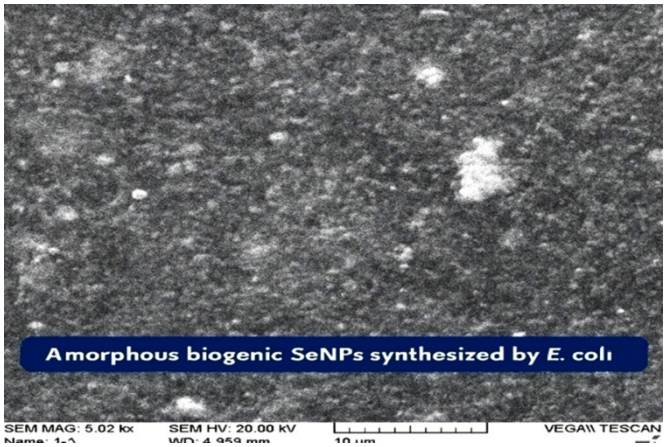

Table 3. Susceptibility of the studied isolates to commonly used antimicrobials.

Antibiotic (code)	S (n, %)	I (n, %)	R (n, %)
Meropenem (MEM)	35 (100%)	0 (0%)	0 (0%)
Ciprofloxacin (CIP)	9 (25.71%)	18 (51.43%)	9 (25.71%)
Ertapenem (ERT)	35 (100%)	0 (0%)	0 (0%)
Trimethoprim–Sulfamethoxazole (SXT)	35 (100%)	0 (0%)	0 (0%)
Ampicillin (AM)	0 (0%)	0 (0%)	35 (100%)
Ceftriaxone (CRO)	0 (0%)	0 (0%)	35 (100%)
Chloramphenicol (C)	35 (100%)	0 (0%)	0 (0%)
Tetracycline (TE)	35 (100%)	0 (0%)	0 (0%)

S: susceptible; I: intermediate; R: resistant; n: number; %: percentage.

Biofilm formation

Most of the *Salmonella* isolates showed that very clear biofilm formation was possible. Out of these examined isolates, 20 (57.1%) were classified as strong biofilm producers, accounting for the majority of tested strains. Moderate biofilm production was observed in 14 isolates (40%) and only 1 isolate (2.9%) showed weak to minimal biofilm formation. None of the isolates were non-biofilm producers. These findings show that the majority of isolates were biofilm producers, which may assist in environmental persistence and resilience against the impact of adverse conditions, such as an antimicrobial agent. The high preponderance of moderate and strong biofilm producers highlights the potential clinical relevance of the strains with respect to chronic or recurrent infection and the propagation of antimicrobial resistance.

Figure 3. Quantitative real-time PCR results of *phoP* and *bapA* genes; the pictures were taken directly from the device.

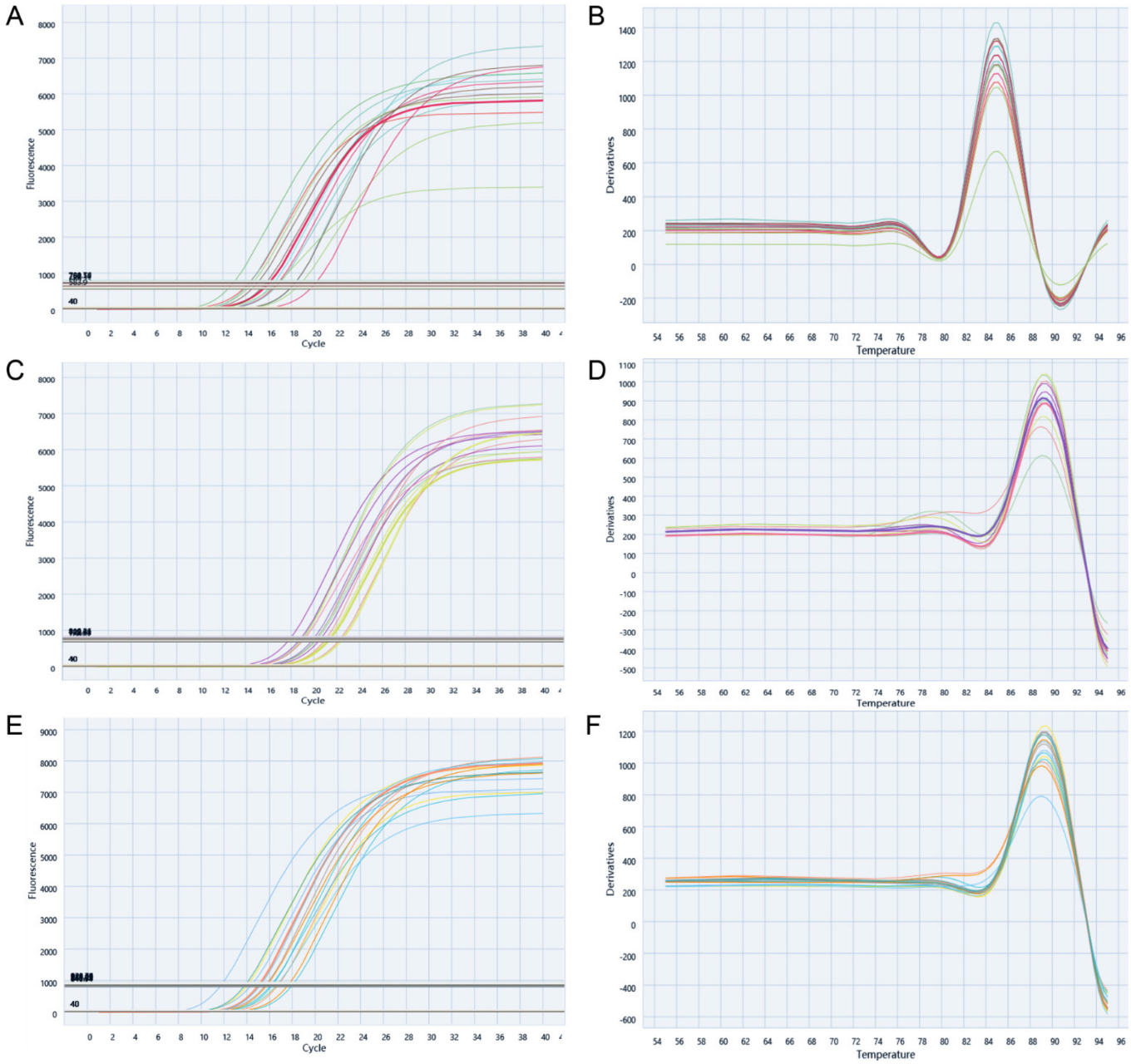

A: Amplification curve of the *phoP* gene with Ct range (14.14–20.22). **B:** Disassociation curve of the *phoP* gene. **C:** Amplification curve of the *bapA* gene with Ct range (18.49–22.66). **D:** Disassociation curve of the *bapA* gene. **E:** Amplification curve of the HKG *gapA* gene with Ct range (14.46–16.95). **F:** Melting curve of the HKG *gapA* gene.

Characterization of SeNPs

Analysis of the absorption spectrum of SeNPs synthesized by *E. coli* using UV–vis spectrometer showed that the absorption band range was around 200–300 nm. This is the spectrum commonly observed in amorphous elemental Se^0 nanoparticles. The absence of any distinct surface plasmon resonance peak confirms the semiconductor nature of selenium and differentiates it from metallic nanoparticles such as gold or silver. The spectra exhibited a gradual degradation in absorbance toward the visible part, and a long absorption tail up to 1000 nm, due to the light scattering of polydisperse particles and due to bacterial biomolecules serving as stabilizing/containing agents of the spectrum. This spectral profile was in line with biological SeNP synthesis of amorphous-sized semi-particle components that are generally at least around 20–200 nm in size with aggregation. The UV–vis absorption spectrum of biosynthesized SeNPs is shown in Figure 1 and the scanning electron microscopy (SEM) micrographs of amorphous biogenic SeNPs derived from *E. coli* are shown in Figure 2.

Molecular study

A clear and gradual change in the levels of *phoP* and *bapA* gene expression was observed following addition of the SeNPs. The expression levels for both the genes showed a significant decrease with increasing concentration of the nanomaterials, compared to the control. Control samples demonstrated the most elevated expression of the genes, gradually decreasing at 12.5, 25, 50, and 100 µg/mL concentrations, which suggested an inverse association between higher concentrations of nanomaterial and higher expression levels of the gene.

The relative expression levels of the target genes (*phoP* and *bapA*) and house-keeping gene were evaluated using RT-qPCR. The amplification profiles and melting curve analyses confirmed the specificity and efficiency of the primers used in this study (Figure 3). The fold expression values were determined utilizing ΔΔCt, and *gapA* was used as a housekeeping gene for accurate measurement. As shown in Table 4, the differences in the expression levels of the *phoP* and *bapA* genes between the control group and groups treated with different concentrations of the nanomaterial were significant. The changes in the

Figure 4. Difference in fold expression of the *phoP* gene among different selenium nanoparticle (SeNP) concentrations.

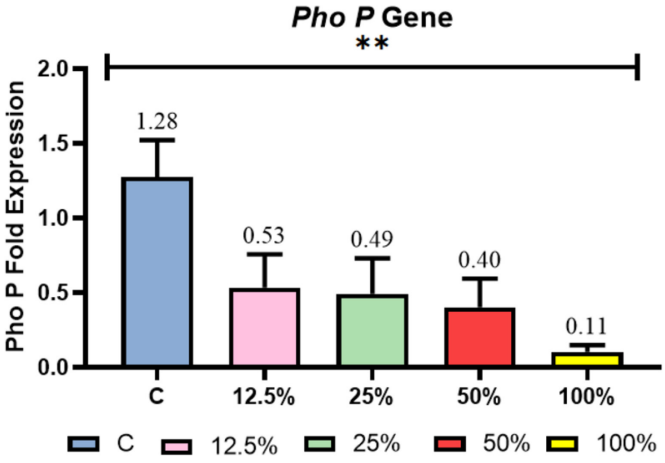

Figure 5. Difference in fold expression of the *bapA* gene among different selenium nanoparticle (SeNP) concentrations.

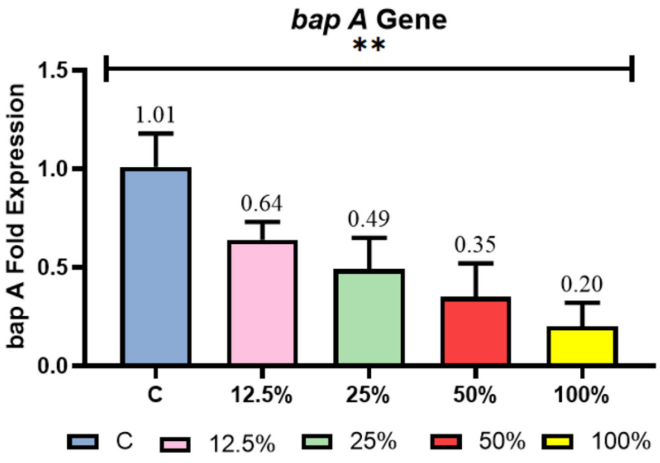

Table 4. Fold expression difference of *phoP* and *bapA* genes in different concentrations of selenium nanoparticles (SeNPs).

Gene	Group	Mean ± SD*	95% CI (lower–upper)	*p* value
pho P	C	1.276 ± 0.246 (C)	0.66–1.89	0.0001**
	12.5	0.534 ± 0.223 (B)	- 0.02–1.09	
	25	0.492 ± 0.239 (B)	- 0.10–1.08	
	50	0.402 ± 0.192 (AB)	- 0.07–0.88	
	100	0.105 ± 0.045 (A)	- 0.01–0.22	
bap A	C	1.009 ± 0.172 (D)	0.58–1.44	0.0001**
	12.5	0.639 ± 0.093 (C)	0.41–0.87	
	25	0.489 ± 0.158 (BC)	0.10–0.88	
	50	0.347 ± 0.170 (AB)	- 0.07–0.77	
	100	0.198 ± 0.116 (A)	- 0.09–0.49	

*A, B, C, D: different letters within a column for each gene denote statistically significant differences ($p < 0.05$) based on Duncan's post-hoc test.

expression of *PhoP* and *bapA* genes varied with the different concentrations of SeNPs (Figures 4 and 5). One-way ANOVA was used to analyze the data to find an overall difference between groups and Duncan's post-hoc test was used to investigate the specific contributors to the variation. The letters accompanying the mean ± SD values represent the Duncan grouping, where groups sharing the same letter are considered statistically non-significant, while those labeled with different letters indicate a statistically significant difference. This classification has been confirmed. Expression levels of the control group were the highest for both *phoP* and *bapA*, while a dramatic and progressive suppression of expression of the genes occurred with increasing concentrations of the nanomaterial (12.5, 25, 50, and 100 µg/mL). The 95% confidence intervals were in agreement with this decline, and the highly significant *p* value (0.0001) indicated a very high dose-dependent inhibition of the expression of both genes. This shows that the concentration of the nanomaterial was inversely correlated with gene expression.

Pearson's correlation analysis (Figure 6) revealed a strong positive correlation between *phoP* and *bapA* gene expression ($r = 0.899$, $n = 15$, $p < 0.001$). The correlation coefficient showed that higher levels of *phoP* were reliably related to higher levels of expression of *bapA*. Regarding the shared variance ($r^2 = 0.807$) that occurred, 81% of the variance in *bapA* expression could be attributed to the *phoP* (consistent with the regression estimation). Covariance analysis (0.12), and test statistic ($t = 7.38$, $df = 13$, $p < 0.001$) were also consistent with the direction dependence of the two genes. Indeed, this strong linear correlation lends support for the regulatory effect of *phoP* on *bapA* by associating both environmental sensing and stress-specific signaling by *phoP* with the transcriptional action of *bapA*, another gene involved in adhesion or biofilm-associated persistence in *Salmonella*.

Linear regression analysis revealed a robust and significant correlation between *phoP* and *bapA* gene expression (Figure 7). Overall, the regression model was significant, $F(1,13) = 54.49$, < 0.001, which accounted for 81% of the variance in *bapA* expression ($R^2 = 0.81$). The regression equation was defined as $\hat{Y} = 0.17 + 0.65X$, suggesting a 0.65 unit increase in *bapA* expression *p* for each unit increment in *phoP*. The slope coefficient ($\beta = 0.65$, $p < 0.001$) and intercept ($\alpha = 0.17$, $p = 0.015$) were statistically significant, indicating that baseline *bapA* expression existed at low *phoP* concentration and that *phoP* appeared as a robust positive *bapA* induction predictor. In terms of biochemistry, these results indicated that regulatory factors derived from *phoP* were strongly responsible for modulating *bapA* expression, which further supports the role of this in linking stress-adaptive signaling with adhesion-associated gene regulation in *Salmonella*.

Discussion

The present investigation illustrates the biosynthesis of SeNPs with *E. coli* and their antibacterial potential against *S. Typhi*. The growing worldwide problem of resistance to antibiotics, especially among enteric pathogens, is highlighted by the realization of these findings and also represents an important first step for the discovery of alternative therapeutic agents. Extensive studies show that biosynthesized SeNPs have significant antibacterial actions causing membrane disruption and subsequent oxidative stress reactions. In these cases [20], similar to the present study, plant-derived SeNPs exhibited mild inhibitory levels against enteric bacteria as a result of marked disruption of bacterial membrane integrity and permeability. In vivo studies [20] have also shown the ability of SeNPs to suppress the colonization of bacteria in gut tissues while preserving intestinal architecture and reducing inflammatory reactions mainly by reducing pro-inflammatory cytokines like IL-6 and IL-1β. Together, these surveys support the emerging view that SeNPs constitute a suitable alternative pathogen

Figure 6. Pearson's correlation analysis between *phoP* and *bapA*.

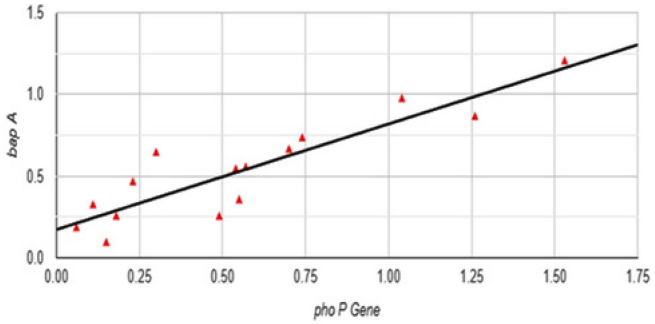

Figure 7. Linear regression analysis between *phoP* and *bapA*.

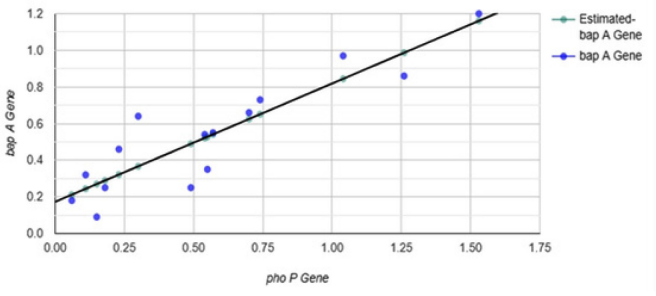

approach, more so in the setting of increased antibiotic resistance [20].

A previous study by Abd *et al*. examined the antimicrobial activity of SeNPs against biofilm-related genes in multidrug-resistant *S. enterica* serovars, including *S. Typhi* [21]. The authors reported that clinical isolates displayed high levels of β-lactamase activity and widespread resistance to commonly used antibiotics, particularly tetracycline and trimethoprim–sulfamethoxazole. Most isolates were strong biofilm producers on plastic surfaces, highlighting their potential role in infection persistence and food safety risks. Notably, the study showed that combining SeNPs with conventional antibiotics produced a synergistic effect, enhancing antimicrobial efficacy. Furthermore, exposure to SeNPs downregulated key biofilm-associated virulence genes such as *adrA*, *gcpA*, and *csgD*.

Another study by Al-Khazraji *et al.* synthesized chemogenic SeNPs using sodium selenite and ascorbic acid, and confirmed that the particles were highly crystalline, spherical, and about 20 nm in size [22]. The SeNPs showed high purity, strong antioxidant activity, and good biocompatibility with no hemolytic effects. Importantly, they exhibited potent antimicrobial activity against *S. enterica* (MIC 16 μg/mL) and strong antibiofilm effects, especially when combined with tetracycline, achieving over 80% inhibition, highlighting that SeNPs are promising antimicrobial and antioxidant agents capable of enhancing conventional antibiotics and helping to overcome bacterial resistance. Al-Roomi and Ajeel reported that among human diarrheal cases *Salmonella* species were the most common pathogens; the two predominant species were *S. Typhi* (48.33%) and *S. paratyphi* (21.67%) [23]. All *S. Typhi* isolates developed robust biofilms, while antibiotic analysis disclosed complete resistance to ticarcillin and strong resistance to aztreonam (89.7%). The study demonstrated that SeNPs synthesized using cinnamon extract showed greater antibacterial activity against *S. Typhi* than the extract alone, achieving a 14.33 mm inhibition zone at 100 μg/mL, compared to 10.66 mm for the extract. These findings highlight the potential of SeNPs as an alternative strategy against multidrug-resistant *S. Typhi.*

In addition, in *Salmonella* Typhimurium, acid stress–induced multi-stress adaptation is orchestrated by the PhoP/PhoQ pathway, and consequently, the observed dose-dependent reduction in phoP following nanomaterial treatment diminishes this adaptive pathway. PhoQ detects low pH, low Mg^{2+}, and cationic antimicrobial peptides; and then induces PhoP to modulate tolerance and virulence genes such as *mgtA, pmrD*, and *pagP*. Low expression of *phoP* likely mitigates Mg^{2+} homeostasis, PmrA/PmrB-dependent lipopolysaccharide (LPS) rearrangement, and RpoS stabilization. Such mechanistic interlinkage is in line with lower survival after acid pre-adaptation and loss of temporary cross-protection under heat and osmotic stress relying on PhoP/PhoQ signaling [24]. The significant decrease of gene expression mediated by the nanomaterial was not restricted to an inhibition in the PhoP/Q pathway but also to its controlling pathway, particularly, the PmrA/B system. While the PhoP/Q system is known for its adverse effects on bacterial motility, its inhibition could theoretically enhance bacterial motility. More importantly, the inhibition of this master regulator (*phoP*) will impair the bacterial cell's ability to adapt its surface charge and resistance to antimicrobial peptides; an important activity for host survival. Thus, the SeNPs not only interfere with a targeted resistance route; rather, they intervene in a multifaceted regulatory network to render the bacteria vulnerable to antimicrobials, thus accounting for the observed reduction in viability in this study [25]. The results show that the SeNPs used negatively regulated gene expression of the master virulence regulator *phoP* in *Salmonella* using a dose-dependent mechanism. This effect is far beyond the typical antibacterial action with the new potential strategy of chemical attenuation of *Salmonella*.

The nanomaterial used in this study is designed to dynamically modulate bacterial virulence, offering a controllable alternative to permanent genetic deletion for rendering bacteria safe for therapeutic applications. This can provide a higher degree of control and safety in the application range for *Salmonella*-mediated cancer treatment, such as in *Salmonella*-mediated cancer, where the severity of attenuation can be increased and decreased by modifying the content of the nanomaterial. This is a promising development in bacterial drug delivery systems [26]. The findings, which prove the effect of the nanomaterial against *Salmonella* on *phoP* gene expression inhibition, are consistent with an international trend to utilize nanoparticles against resistant bacteria. The recently reported biogenic silver nanoparticles were able to kill strains of multidrug-resistant *S. enterica* with a high level of efficiency. Although earlier research had pointed out the structural damage induced by SeNPs, such as injury of the bacterial membrane, the current study adds a complementary molecular contribution by showing an intervention mechanism by the disturbance of the virulence regulatory network. The integration of

direct structural action and regulatory gene suppression may explain the high potency of the SeNPs and may provide new methods to design more selective and effective medications to overcome resistance to pathogens [27].

In addition to its effect on virulence regulators like phoP, the results of this study reveal that the SeNPs significantly downregulate the expression of *bapA*, a key gene responsible for biofilm formation in *Salmonella*, which agrees with a previous study [28] that demonstrated that biofilms provide bacteria with a protective shield against antibiotics and the host's immune response. Therefore, the observed decrease in *bapA* expression suggests that the nanomaterial impairs *Salmonella's* ability to form these resilient communities, rendering them more susceptible to clearance, by inhibiting virulence and preventing biofilm formation; this highlights the promising potential of the nanomaterial as an effective therapeutic agent against persistent bacterial infections.

The ability of clinical *Salmonella* isolates to form biofilms is a key virulence trait, strongly correlated with the presence of specialized genes like *bapA* and *csg*. Phenotyping and genotyping studies have demonstrated that the majority of pathogenic strains possess this capability. In this context, this study showed a dose-dependent inhibition of *bapA* expression by the SeNPs. Crucially, this downregulation occurred at sub-minimum inhibitory concentrations (sub-MIC), suggesting that the SeNPs specifically target the molecular machinery of biofilm formation rather than merely inhibiting overall bacterial growth. This implies that the nanomaterial can potentially convert a strong biofilm-producing strain into a weak or non-producing one, thereby dismantling its protective fortress and rendering it vulnerable to therapies and immunity. This represents an effective strategy for combating persistent infections [29].

The findings demonstrating that SeNPs inhibit *bapA* expression are in strong agreement with other studies that have explored the impact of nanoparticles on biofilm regulatory networks. A recent investigation demonstrated that modulation of biofilm-associated gene expression is a common and effective antimicrobial mechanism of SeNPs against resistant bacteria [30]. SeNPs significantly downregulated *csgD* and *adrA*, the central regulators of biofilm matrix synthesis in *Salmonella*. Since *csgD* functions as a master regulator and *bapA* encodes a major structural biofilm component, these observations indicate that SeNPs, irrespective of their specific formulation, disrupt biofilm development on multiple fronts by targeting both upstream regulatory pathways and crucial structural elements.

The dose-dependent suppression of *phoP* and *bapA* by SeNPs suggests that this nanomaterial modulates *S. Typhi* at the regulatory level rather than acting purely through growth inhibition or killing. By simultaneously targeting a central virulence regulator and a key biofilm gene, SeNPs likely reduce the bacterium's ability to adapt to host stress, establish robust biofilms, and resist standard antimicrobial agents. These results align with evidence that nanoparticles can affect both free-living and biofilm-associated bacteria and, together with the preserved susceptibility to several non–β-lactam drugs, support the use of SeNPs as promising adjuncts in combination regimens against MDR *Salmonella*.

Nevertheless, several limitations should be considered. The study was restricted to a single center and included only 35 isolates, which may constrain the broader applicability of the findings. All assays were performed under in vitro conditions, leaving the in vivo pharmacodynamics, toxicity, and therapeutic potential of SeNPs unresolved. Moreover, the analysis focused exclusively on two virulence-associated genes, without incorporating genome-wide expression or proteomic profiling that could identify broader regulatory impacts or compensatory pathways. Finally, the long-term ecological and safety consequences of nanoparticle use, including effects on host microbiota and environmental systems, were not assessed and warrant further investigation.

Conclusions

The current findings show that biosynthesized SeNPs exhibit very active and dose-dependent inhibiting effects on antibiotic-resistant *S. Typhi* through downregulation of the virulence regulator *phoP* and the biofilm-associated gene *bapA*, to attenuate pathogenicity and biofilm flexibility in strains with complete β-lactam resistance. The high and positive correlation between the two genes ($r = 0.899$) serves to demonstrate integrated regulatory pathways that are targeted via SeNPs and render SeNPs an attractive auxiliary element with the potential to improve the activity of conventional antibiotics, such as carbapenems and chloramphenicol. While promising, the results should be treated carefully based on their single-center design, limited isolate numbers, and in vitro-based use in the study. Further studies should involve validation in animal models, comprehensive safety profiling, and use of combination therapy routines (including more extensive transcriptomic or proteomic analyses) to further clarify the regulatory

influences of SeNPs and facilitate their translation to clinical use in the treatment of long-lasting and drug-resistant typhoid infections.

Acknowledgements

We sincerely thank all participants who provided samples for this study. We also gratefully acknowledge the support of the Iraqi Hereditary Company (IHC) for their assistance with the practical aspects of this work.

Corresponding author

Huda Abbas Abd, MSc
University of Information Technology and Communications (UOITC)
Al-Nidhal Street, Baghdad 10011, Iraq.
Tel: +964 771 906 5294
Email: hudaa2348@gmail.com; huda.abbas@uoitc.edu.iq

Conflict of interest

No conflict of interest is declared.

References

1. Bayda S, Adeel M, Tuccinardi T, Cordani M, Rizzolio F (2019) The history of nanoscience and nanotechnology: from chemical-physical applications to nanomedicine. Mol Basel Switz 25: 112. doi: 10.3390/molecules25010112.
2. Mikhailova EO (2023) Selenium nanoparticles: green synthesis and biomedical application. Mol Basel Switz 28: 8125. doi: 10.3390/molecules28248125.
3. Husain S, Sultan RMS, Saxena K, Bano F, Goyal R, Chopra S, Chopra H, Verma SK (2025) Nano selenium: a promising solution for infectious diseases — current status and future prospects. Curr Pharm Des 31: 2795–2819. doi: 10.2174/0113816128346637250401090138.
4. Laib I, Gheraissa N, Benaissa A, Benkhira L, Azzi M, Benaissa Y, Abdelaziz AG, Tian F, Walsh M, Bechelany M, Barhoum A (2025) Tailoring innovative silver nanoparticles for modern medicine: the importance of size and shape control and functional modifications. Mater Today Bio 33: 102071. doi: 10.1016/j.mtbio.2025.102071.
5. Kora AJ, Rastogi L (2017) Bacteriogenic synthesis of selenium nanoparticles by *Escherichia coli* ATCC 35218 and its structural characterisation. IET Nanobiotechnol 11: 179–184. doi: 10.1049/iet-nbt.2016.0011.
6. Han J, Aljahdali N, Zhao S, Tang H, Harbottle H, Hoffmann M, Frye JG, Foley SL (2024) Infection biology of *Salmonella enterica*. EcoSal Plus 12: eesp00012023. doi: 10.1128/ecosalplus.esp-0001-2023.
7. Latasa C, Roux A, Toledo-Arana A, Ghigo J, Gamazo C, Penadés JR, Lasa I (2005) BapA, a large secreted protein required for biofilm formation and host colonization of *Salmonella enterica* serovar *Enteritidis*. Mol Microbiol 58: 1322–1339. doi: 10.1111/j.1365-2958.2005.04907.x.
8. Guttula D, Yao M, Baker K, Yang L, Goult BT, Doyle PS, Yan J (2019) Calcium-mediated protein folding and stabilization of *Salmonella* biofilm-associated protein A. J Mol Biol 431: 433–443. doi: 10.1016/j.jmb.2018.11.014.
9. Groisman EA, Duprey A, Choi J (2021) How the PhoP/PhoQ system controls virulence and Mg^{2+} homeostasis: lessons in signal transduction, pathogenesis, physiology, and evolution. Microbiol Mol Biol Rev 85: e0017620. doi: 10.1128/MMBR.00176-20.
10. Aguirre A, Cabeza ML, Spinelli S V, McClelland M, García Véscovi E, Soncini FC (2006) PhoP-induced genes within *Salmonella* pathogenicity island 1. J Bacteriol 188: 6889–6898. doi: 10.1128/JB.00804-06.
11. Mao M, He L, Yan Q (2025) An updated overview on the bacterial PhoP/PhoQ two-component signal transduction system. Front Cell Infect Microbiol 15: 1509037. doi: 10.3389/fcimb.2025.1509037.
12. Aga AM, Mulugeta D, Muleta D, Woldesemayat AA, Motuma A, Kelel M, Wakitole B, Tadesse S, Teferi Z, Woldemariyam FT, Oljira S, Ferede H, Berihun N, Girma S, Nigussie D, Tafesse Gemeda M (2025) Antibiotic susceptibility patterns of *Salmonella* isolates from clinical, food, and environmental sources in Addis Ababa and surrounding towns, Ethiopia. Microbiol Spectr 13: e00970–25. doi: 10.1128/spectrum.00970-25.
13. Agarwal RK, Singh S, Bhilegaonkar KN, Singh VP (2011) Optimization of microtitre plate assay for the testing of biofilm formation ability in different *Salmonella* serotypes. Int Food Res J 18: 1493.
14. Shatila F, Yaşa İ, Yalçın HT (2021) Biofilm formation by *Salmonella enterica* strains. Curr Microbiol 78: 1150–1158. doi: 10.1007/s00284-021-02373-4.
15. Khaddam W, Durgham B (2025) Comparative analysis of biofilm detection methods and antibiotic resistance in catheter-associated uropathogens: a cross-sectional study from Syria. BMC Microbiol 25: 760. doi: 10.1186/s12866-025-04506-2.
16. Al-Khafaji HMA-A, Khadum RM, Ouda SM, Mohammed MQ (2025) Inverse correlation of miR-196a and HOXB13 expression in Iraqi patients with prostate cancer. Cell Mol Biol 71: 63–70. doi: 10.14715/cmb/2025.71.9.8.
17. Al-Kafagi HMA-A, Hussein NNA, Mohammed MQ, Hussein ZA, Al-Tameemi AKA (2025) The correlation between gene expression of growth differentiation factor 9B (GDF9B) gene and miR-378-5p in infertile women. Iraqi J Sci 66: 1560–1569. doi: 10.24996/ijs.2025.66.4.15.
18. Muhammed HJ, Al-Attar MM, Shubrem ZF, Al-Saedi MKA, Mohammed MQ (2025) Quantitative real-time PCR analysis of circulating microRNA levels in blood samples from pediatric patients with epilepsy. Gene Rep 39: 102214. doi: 10.1016/j.genrep.2025.102214.
19. Faris AZ, Sadoon HA, Qasim MM, Aneed A-SMK, Abdal A-TAK (2024) The role of CD279 and CD274 gene polymorphisms in Iraqi patients with multiple sclerosis by using real-time qPCR HRM technique. Res J Biotechnol 19: 11. doi: 10.25303/1911rjbt2370243.
20. Saleh A, El-Masry TA, Negm WA, Alotaibi B, Elharty ME, Alotaibi KN, Elekhnawy E (2023) Unravelling the antibacterial potential of biosynthesized selenium nanoparticles against *Salmonella Typhimurium* food pathogen: in vitro and in vivo investigation. Eur Rev Med Pharmacol Sci 27: 3631–3644. doi: 10.26355/eurrev_202304_32149.
21. Abd MA, Al-Quhli SQ, Jassim MA (2024) Assessment of the effect of selenium nanoparticles on the expression of virulence genes *csgD*, *adrA*, and *gcpA* of multidrug-resistant *Salmonella enterica*. Prevention 5: 6. doi: 10.37652/juaps.2024.146103.1178.

22. Al-Khazraji ZAH, Kadhim MJ, Ahmed ME (2025) The biological activity of chemogenic selenium nanoparticles on *Salmonella enterica* isolated from clinical cases. SAR J Pathol Microbiol 6: 179–185. doi: 10.36346/sarjpm.2025.v06i04.006.
23. Al-Roomi NM, Ajeel HH (2024). Antibacterial effect of green synthesis of selenium nanoparticles against *Salmonella typhi* in small buffalo. Uttar Pradesh Journal of Zoology 45: 80–90. doi: 10.56557/upjoz/2024/v45i53933.
24. Gao X, Han J, Zhu L, Nychas G-JE, Mao Y, Yang X, Liu Y, Jiang X, Zhang Y, Dong P (2024). The effect of the PhoP/PhoQ system on the regulation of multi-stress adaptation induced by acid stress in *Salmonella Typhimurium*. Foods 13: 1533. doi: 10.3390/foods13101533.
25. Shprung T, Wani NA, Wilmes M, Mangoni ML, Bitler A, Shimoni E, Sahl H-G, Shai Y (2021) Opposing effects of PhoPQ and PmrAB on the properties of *Salmonella enterica* serovar *Typhimurium*: implications on resistance to antimicrobial peptides. Biochemistry 60: 2943–2955. doi: 10.1021/acs.biochem.1c00287.
26. Becerra-Báez EI, Meza-Toledo SE, Muñoz-López P, Flores-Martínez LF, Fraga-Pérez K, Magaño-Bocanegra KJ, Juárez-Hernández U, Mateos-Chávez AA, Luria-Pérez R (2022) Recombinant attenuated *Salmonella enterica* as a delivery system of heterologous molecules in cancer therapy. Cancers 14: 4224. doi: 10.3390/cancers14174224.
27. Estevez MB, Casaux ML, Fraga M, Faccio R, Alborés S (2021) Biogenic silver nanoparticles as a strategy in the fight against multi-resistant *Salmonella enterica* isolated from dairy calves. Front Bioeng Biotechnol 26: 644014. doi: 10.3389/fbioe.2021.644014.
28. Silva-Hidalgo G, López-Valenzuela M, Cárcamo-Aréchiga N, Cota-Guajardo S, López-Salazar M, Montiel-Vázquez E (2016) Identification of *bapA* in strains of *Salmonella enterica* subsp. *enterica* isolated from wild animals kept in captivity in Sinaloa, Mexico. Vet Med Int 2016: 3478746. doi: 10.1155/2016/3478746.
29. Shalal S, Jaber N, Hussein K (2022) Phenotyping and genotyping of *Salmonella enterica* as biofilm producer isolated from diarrheal animal and human. Basrah J Vet Res 21: 24–35. doi: 10.23975/bjvetr.2022.176611.
30. Abd MA, Al-Quhli SQ, Jassim MA (2024) Assessment of the effect of selenium nanoparticles on the expression of virulence genes *csgD*, *adrA*, and *gcpA* of multidrug-resistant *Salmonella enterica*. prevention 18: 5–6. doi: 10.37652/juaps.2024.146103.1178.